

Graphicality of power-law and double power-law degree sequences

Pietro Valigi,¹ M. Ángeles Serrano,^{2,3,4} Claudio Castellano,⁵ and Lorenzo Cirigiano¹

¹*Dipartimento di Fisica Università La Sapienza, I-00185 Rome, Italy*

²*Department of Condensed Matter Physics, University of Barcelona, E-08028 Barcelona, Spain*

³*University of Barcelona Institute of Complex Systems (UBICS), E-08028 Barcelona, Spain*

⁴*Institució Catalana de Recerca i Estudis Avançats (ICREA), E-08010 Barcelona, Spain*

⁵*Istituto dei Sistemi Complessi (ISC-CNR), Via dei Taurini 19, I-00185 Rome, Italy*

(Dated: January 1, 2026)

The graphicality problem – whether or not a sequence of integers can be used to create a simple graph – is a key question in network theory and combinatorics, with many important practical applications. In this work, we study the graphicality of degree sequences distributed as a power-law with a size-dependent cutoff and as a double power-law with a size-dependent crossover. We combine the application of exact sufficient conditions for graphicality with heuristic conditions for nongraphicality which allow us to elucidate the physical reasons why some sequences are not graphical. For single power-laws we recover the known phase-diagram, we highlight the subtle interplay of distinct mechanisms violating graphicality and we explain why the infinite-size limit behavior is in some cases very far from being observed for finite sequences. For double power-laws we derive the graphicality of infinite sequences for all possible values of the degree exponents γ_1 and γ_2 , uncovering a rich phase-diagram and pointing out the existence of five qualitatively distinct ways graphicality can be violated. The validity of theoretical arguments is supported by extensive numerical analysis.

I. INTRODUCTION

Given a collection of integer numbers $\underline{k} = (k_1, \dots, k_N)$, can we build an undirected simple graph having \underline{k} as degree sequence? This is the problem of *graphicality*, a fundamental question in graph theory with implications in the modeling of real networks, the verification of observed data, and the detection of anomalies in experiments. A trivial necessary condition for graphicality is the *handshaking lemma*: the sum of all the integers must be an even number $\sum_{i=1}^N k_i = 2E$, with $E \geq 0$ being the number of edges. A second trivial necessary condition is that $k_i \leq N - 1$ for each i . If that is not the case, one cannot create a simple graph. For these reasons, we focus only on sequences with an even sum and in which each k_i is at most $N - 1$.

A vast literature exists on the graphicality problem [1–9], identifying non-trivial necessary and sufficient conditions for a sequence to be graphical. Some of these results can be used to analyze the graphicality of power-law distributed degree sequences, which play a central role in the theory of complex networks and their applications. The Erdős-Gallai (EG) theorem states that an ordered non-increasing degree sequence $\underline{k} = (k_1, \dots, k_N)$, with even sum, is graphical if and only if

$$\sum_{i=1}^n k_i \leq n(n-1) + \sum_{i=n+1}^N \min\{n, k_i\}, \quad (1)$$

for all $1 \leq n \leq N$ [1]. In other words, the demand for connections among the top degree nodes cannot exceed the supply of available connections from the rest of the graph and among themselves. If one of the inequalities fails, then some of the high-degree nodes cannot be satisfied. If all the inequalities hold, then the sequence is graphical. To actually build a graph from a degree sequence, several

algorithms exist [10–20]. The Havel–Hakimi (HH) theorem [21, 22] provides one of these constructive algorithms. It states that an ordered non-increasing degree sequence $\underline{k} = (k_1, \dots, k_N)$, with even sum, is graphical if and only if the sequence $\underline{k}' = (k_2 - 1, k_3 - 1, \dots, k_{k_1} - 1, \dots, k_N)$ is graphical. Hence, one can build the graph by connecting the node with the largest degree to the nodes with the next highest degrees, then reduce their corresponding degrees and repeat the process until all degrees are zero, which would imply graphicality, or a contradiction arises.

By using these theorems, which hold for any degree sequence, Del Genio et al. [23] analyzed the graphicality of degree sequences sampled from a power-law degree distribution, $p_k \sim k^{-\gamma}$, when the maximum possible degree k_c is unbounded, being limited only by the system size $k_c = N - 1$. In this way they concluded that, in the infinite size limit, the fraction of graphical degree sequences vanishes for $0 < \gamma < 2$, implying that all realizable scale-free networks are necessarily sparse. The infinite size limit can however be reached in a more general way, imposing a sharp upper cutoff depending on the system size as $k_c = (N - 1)^{1/\omega}$ with $\omega \geq 1$. In such scenario, again by applying the EG theorem, Baek et al. [24] showed that graphicality is guaranteed for $\omega > \gamma$ if $\gamma < 2$ and for any ω if $\gamma > 2$.

Previous works provide the correct solution of the problem of graphicality for infinite power-law distributed networks. However the physical origin of the various regimes remains not clear. Moreover numerical results on finite networks converge in a surprisingly slow manner to the behavior predicted in the infinite size limit. In this work, we reanalyze the problem of graphicality of power-law distributed networks, providing a physical interpretation of the nature of the various regions of the phase-diagram. In this way, we also understand the origin of the slow approach to the infinite size limit. In addition, we extend

the analysis to degree-sequences distributed according to a double power-law, which are often found both in models [25, 26] and in empirical investigations [27–30]. In such a case, we reveal a remarkably rich and intriguing phenomenology, with various different mechanisms underlying the violations of graphicality.

The rest of this paper is organized as follows: In Sec. II we present sufficient conditions for graphicality and heuristic criteria for nongraphicality; we apply such criteria to single power-law sequences in Sec. III and to double power-law sequences in Sec. IV, comparing with the results of numerical simulations; finally, we discuss our findings in Sec. V.

II. CONDITIONS FOR GRAPHICALITY

In this section, we present the sufficient conditions for graphicality and nongraphicality that will be used later in the analysis of single and double power-law networks.

A. Sufficient conditions for graphicality

The Erdős-Gallai and Havel-Hakimi theorems provide necessary and sufficient conditions for graphicality involving all degrees in the sequence. Two other exact results provide instead sufficient criteria for graphicality at a more "coarse-grained" level, based on the consideration of only a few of the sequence features.

Zverovich and Zverovich (ZZ) [31] have shown that if the following inequality holds

$$N \geq \frac{(k_{\max} + k_{\min} + 1)^2}{4k_{\min}}, \quad (2)$$

then the sequence is graphical.

The ZZ condition has been later generalized by Cloteaux [32], who showed that if

$$(k_{\max} - k_{\min}) \left(\frac{N - k_{\max} - 1}{Nk_{\max} - S} + \frac{k_{\min}}{S - Nk_{\min}} \right) \geq 1, \quad (3)$$

then the sequence is graphical. Here $S = \sum_i k_i = N\langle k \rangle$ is the number of stubs, i.e., half-edges. Notice that Cloteaux's bound is stronger than the ZZ condition, and it can certify graphicality in sequences where ZZ fails. Still, it is only a sufficient condition, not necessary.

B. Sufficient conditions for nongraphicality

The exact results presented above can be complemented by additional, more physical, arguments, which provide heuristic sufficient conditions determining when degree sequences are not graphical. In this way, we clarify the physical origin of the nongraphicality of sequences. They are inspired by the Erdős-Gallai and Havel-Hakimi theorems.

A first condition is based on the asymptotic scaling of the number of stubs as a function of N . The general idea is the following. Nodes can be divided in categories, depending on their degree. For example, for single power-law sequences, there are nodes whose degree is finite $k = \mathcal{O}(1)$ and those with degree growing with N , which we call *hubs*. In the case their degree is $k = \mathcal{O}(N)$ we refer to them as *superhubs*. The scaling of the number of stubs attached to each type of node with system size N can be determined as a function of the parameters of the degree distribution. Similarly, it is possible to compute the scaling of the total number of stubs $S = N\langle k \rangle$ from the average degree $\langle k \rangle$. This information allows to determine, for each value of the distribution parameters, which type of nodes accounts for the scaling of the total number of stubs. We dub this category the *dominating* nodes. In general, only one class of node dominates (except at the transition values), and, accordingly, it is necessary to match their stubs with each other for the sequence to be graphical.

Hence the ratio r between the number of stubs emanating from dominant nodes and the square of the number of dominating nodes provides relevant information on the network graphicality. If the ratio diverges with N , it is not possible to pair the stubs of the dominating nodes with each other and the sequence cannot be graphical. If the ratio vanishes with N , these stubs can be paired, at least in principle. Although this is not a sufficient condition for graphicality (as we will see in an example), it points toward graphicality. If the ratio goes to a finite value no conclusion can be drawn. In such a case, if the largest degree is N , it is necessary to consider another condition, directly connected to the Havel-Hakimi algorithm. According to the HH procedure, in the first step one has to connect the node with highest degree k_{\max} , with the k_{\max} following nodes in order of degree. If $k_{\max} = N - 1$ then all other nodes must be connected, including those with smallest degree. If there are nodes with degree 1, their stubs will be used up. If another node has degree $N - 1$ then it is impossible to pair its stubs, because there are less than $N - 1$ nodes with available stubs. We conclude that when there is a finite (or growing) number of nodes of degree $N - 1$ and a finite (or growing) number of nodes of degree 1, the Havel-Hakimi theorem guarantees that the sequence is not graphical. More in general, the HH theorem imposes conditions on the minimum degree given the number of nodes with degree $N - 1$. The same argument can be extended even further: if the number of nodes of degrees of order $\mathcal{O}(N)$ is larger than N^α , for any $\alpha \in [0, 1]$, and the number $\mathcal{N}_{N^\alpha} = Np_{k=N^\alpha}$ of nodes of degree N^α is finite (or growing), then by the Havel-Hakimi algorithm the sequence cannot be graphical, because all the stubs of nodes of degree N^α are needed to connect to a subset of the superhubs and no more stubs are available for connecting to the rest of superhubs.

For simplicity, with a slight abuse of language, we will call this "Havel-Hakimi condition" in the rest of the paper.

III. GRAPHICALITY OF SINGLE POWER-LAW SEQUENCES

We study the graphicality of degree sequences \underline{k} where each k_i is independently drawn from a single power-law (SPL) discrete distribution p_k between k_{\min} and k_c , and exponent γ , such that

$$p_k = \frac{k^{-\gamma}}{Z(\gamma, k_{\min}, k_c)}, \quad (4)$$

where

$$Z(\gamma, k_{\min}, k_c) = \sum_{k=k_{\min}}^{k_c} k^{-\gamma} \quad (5)$$

is the normalization constant.

True power-law distributions are defined only if the heavy tail persists in the $N \rightarrow \infty$ limit: for this reason, we do not consider distributions with a finite upper cutoff $k_c = \mathcal{O}(1)$. We study instead sequences \underline{k} with a size-dependent cutoff $k_c = (N - 1)^{1/\omega}$, with $\omega \geq 1$. The case $\omega = 1$ has already been studied in Ref. [23], while the case $\omega > 1$ has been studied in Ref. [24]. Here, we will reconsider both cases to provide a simple physical interpretation of the origin of those results. The same interpretation will guide us later in the analysis of double power-law sequences. For simplicity, but with no loss of generality, we take $k_{\min} = 1$.

A few remarks are in order. First of all, extreme value theory tells us (see Appendix A) that, sampling from a SPL distribution as in Eq. (4), the expected value k_{\max} of the largest observed degree is $k_{\max} \sim N^{1/(\gamma-1)}$ if $\omega < \gamma - 1$, which corresponds to the *natural cutoff* in an unbounded distribution, and $k_{\max} = k_c$ otherwise. Note that since $\omega \geq 1$, the natural cutoff plays a role only for $\gamma > 2$.

Another useful remark: if a sequence is graphical at a given ω for some γ , then it is graphical for all the $\omega' \geq \omega$. In particular, if a sequence with $\omega = 1$ is graphical then it is graphical for any $\omega > 1$.

In Appendix A we calculate the scaling of the various quantities needed in the following to evaluate the conditions for graphicality or nongraphicality.

A. Sequences with $\omega = 1$

By comparing Eq. A2 and Eq. A6 with Eq. A7 it is immediate to see that the dominating nodes are superhubs if $\gamma < 2$, while finite degree nodes dominate for $\gamma > 2$. In this last case there are order $\mathcal{O}(N)$ stubs that must be paired between order $\mathcal{O}(N)$ nodes and the matching is easily doable. For $\gamma < 2$, instead, hubs dominate and we must compute the ratio $r_{\mathcal{O}(N)} = S_{\mathcal{O}(N)}/\mathcal{N}_{\mathcal{O}(N)}^2$ to check whether it is possible to pair all stubs emanating from

hubs with each other

$$r_{\mathcal{O}(N)} = \frac{S_{\mathcal{O}(N)}}{\mathcal{N}_{\mathcal{O}(N)}^2} = \begin{cases} N^{\gamma-1}, & 1 < \gamma < 2, \\ \mathcal{O}(1), & \gamma < 1. \end{cases} \quad (6)$$

For $\gamma > 1$ the ratio diverges: there are too many stubs emanating from hubs to be paired with each other. As a consequence, sequences are not graphical for $1 < \gamma < 2$. Note that for $\gamma > 2$ it is still impossible to perform this pairing, but stubs from hubs can be paired with stubs from finite degree nodes, which are dominating in that region. For $\gamma < 1$ instead the ratio goes to a finite value as N grows. This may mean that the pairing is possible, but in this case one has to take into account the additional HH condition for nongraphicality (see Sec. II B). In the present case there are N^γ nodes of finite degree. Hence for $\gamma > 0$ the condition implies that sequences are nongraphical, while this is not true for $\gamma < 0$.

In this way we have provided a physical interpretation of the results of Ref. [23]. Sequences are not graphical in the interval of values of γ between 0 and 2, but the physical origin is different if γ is larger or smaller than 1. For $\gamma > 1$ there are far too many stubs emanating from hubs; they cannot be paired with each other and there are too few stubs from finite-degree nodes to match them. For $\gamma < 1$ instead, nongraphicality descends from the simultaneous presence of nodes of finite degree and nodes of degree $N - 1$. This is a much milder violation of graphicality that, as we are about to see, disappears as soon as the largest degree grows more slowly than N .

B. Sequences with $\omega > 1$

The ZZ condition implies graphicality for any γ and $\omega > 2$.

Considering instead Cloteaux's condition in the limit $N \rightarrow \infty$, it implies (see Appendix B for details) that graphicality holds if $\omega > \gamma$, for $1 < \gamma < 2$, and it holds for any $\omega > 1$ for $\gamma < 1$.

Concerning the sufficient conditions for nongraphicality, whenever $\omega > 1$ there are no superhubs and therefore the Havel-Hakimi condition does not apply. Considering the scaling of the number of stubs, for $\gamma > 2$ finite degrees dominate and sequences are trivially graphical. For $1 < \gamma < 2$ hubs dominate instead and the ratio $r_{\mathcal{O}(k_{\max})} = S_{\mathcal{O}(k_{\max})}/\mathcal{N}_{\mathcal{O}(k_{\max})}^2 \sim N^{\frac{\gamma}{\omega}-1}$. Hence, we find that sequences cannot be graphical if $\omega < \gamma$. For $\gamma < 1$ hubs still dominate but the ratio $r_{\mathcal{O}(k_{\max})} \sim N^{\frac{1}{\omega}-1}$. Since the exponent is negative, nongraphicality is not predicted. Indeed, in this region we know that sequences are graphical because of Cloteaux's inequality. These results are summarized in Fig. 1(a).

In this way, we have provided a physical interpretation of the results, reported in Ref. [24], for a power-law degree distribution in the presence of a growing degree cutoff. In particular, it is important to stress the discontinuity occurring for $0 < \gamma < 1$: as soon as ω is larger than 1,

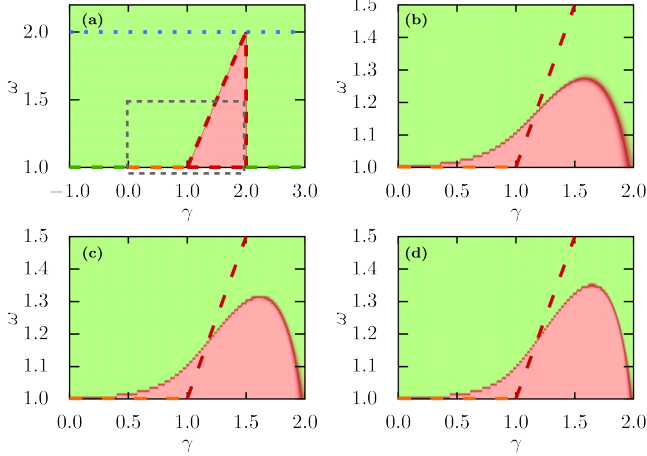


Figure 1. (a) Phase diagram for the graphicality of SPL degree sequences in the limit $N \rightarrow \infty$. Sequences are graphical in green regions, and they are non-graphical in red regions. Above the blue dotted line ZZ condition applies. The line $\omega = 1$ corresponds to the case considered in Ref. [23]. The rest of the phase-diagram is the same of Ref. [24] with their α equal to $1/\omega$ here. Phase diagram for the graphicality of SPL sequences, close to the transition line, obtained from numerical simulations sequences of size (b) $N = 10^5$, (c) $N = 10^6$, (d) $N = 10^7$, compared with the infinite size-limit (grey dashed box in panel (a)). The colors represent the value of $\langle g \rangle$ as a function of γ and ω . Results are averaged over $M = 1000$ independent samples. Note the presence of huge finite-size effects, and the slow convergence to the theoretical prediction for the nongraphical region as N increases.

there are no more hubs with extensive degree (superhubs) and the subtle violation of the Havel-Hakimi condition, represented with an orange dashed line at $\omega = 1$ in Fig. 1(a), disappears. Note also that the regions where sufficient conditions for graphicality and for nongraphicality apply are complementary, thus allowing to fully understand the graphicality problem in the whole phase-diagram.

C. Numerical results

We generate M samples of degree sequences k from power-law distributions with k between $k_{\min} = 1$ and $k_c = N^{1/\omega}$, for various values of ω . For each sequence we check if it is graphical or not by applying Erdős-Gallai theorem, which gives a necessary and sufficient condition (see Appendix C for details). This corresponds to assigning to each sequence a Bernoulli variable $g_t = 1$ if the sequence is graphical, and $g_t = 0$ otherwise. We then compute the average fraction of graphical sequences

$$\langle g \rangle = \frac{1}{M} \sum_{t=1}^M g_t. \quad (7)$$

In Fig. 1(b) we report the value of $\langle g \rangle$ as a function of γ and ω for three system sizes N . As N grows, the

average fraction of graphical sequences tends to conform to the theoretical prediction, with discontinuous transitions separating the different phases, as already reported in Ref. [24]. It is also clear that the reaching of the asymptotic behavior is exceedingly slow. To quantify this convergence to the asymptotic values, we define the effective finite-size transition points $\gamma_-(N)$ and $\gamma_+(N)$, that in the limit $N \rightarrow \infty$, converge to the respective limits $\gamma_-(\infty) = \omega$ and $\gamma_+(\infty) = 2$.

For fixed $\omega > 1$, we can roughly estimate the position of these size-dependent thresholds as follows. The transition from graphical to nongraphical occurring in the infinite-size limit for $\gamma = \omega$ is caused by the impossibility of pairing the hubs among themselves, indicated by a diverging ratio $r_{\mathcal{O}(k_{\max})} \sim N^{\gamma/\omega-1}$. Thus we can estimate the finite-size transition point $\gamma_-(N)$ by setting $r_{\mathcal{O}(k_{\max})} = \mathcal{O}(1)$, which implies a scaling relation of the form

$$\omega - \gamma_-(N) \sim \frac{C_- \omega}{\log(N)}, \quad (8)$$

where C_- is a constant. The other transition, occurring at $\gamma = 2$ in the infinite-size limit, is caused by the impossibility of pairing the stubs of the hubs with the stubs of finite-degree nodes, thus it occurs when $N^{1+\frac{2-\gamma}{\omega}} \gg N$. Setting $N^{\frac{2-\gamma_+(N)}{\omega}} = \mathcal{O}(1)$ implies a scaling relation of the form

$$2 - \gamma_+(N) \sim \frac{C_+ \omega}{\log(N)}, \quad (9)$$

where C_+ is a positive constant.

We tested the scaling relations in Eq. (8) and (9) via a finite-size scaling analysis close to the transition points, for different values of ω , and several values of N . Numerically the finite-size transition points $\gamma_-(N)$ and $\gamma_+(N)$ are identified by the positions of peaks of the variance $\langle \delta g^2 \rangle$ as γ is varied. The results of this finite-size scaling analysis, for three distinct values of ω , reported in Fig. 2 showing a good agreement with a functional form of the type

$$\gamma_{\pm}(\infty) - \gamma_{\pm}(N) \simeq C_{\pm}(\omega) \log(N)^{-a_{\pm}(\omega)}, \quad (10)$$

where C_{\pm}, a_{\pm} are parameters whose value depend on ω , and $a_{\pm} > 0$. In particular, we find that C_- can be either positive or negative, while $C_+ > 0$, in agreement with Fig. 1(b). The numerical findings confirm the logarithmically slow approach to the asymptotic threshold values predicted by the theoretical argument. The preasymptotic corrections appear not in agreement with the predicted inverse logarithmic behavior, although an analysis of the local effective exponents (not shown) suggests that for much larger values of N the scalings in Eqs. (8) and (9) might hold.

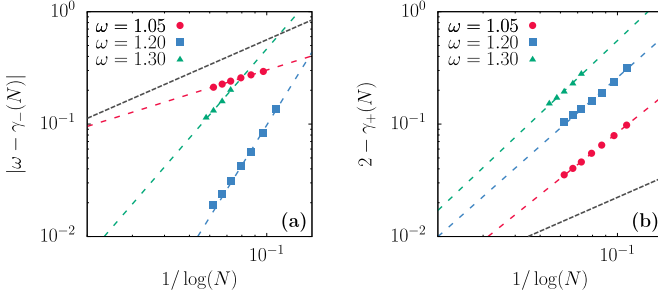


Figure 2. Finite-size scaling analysis of the transition points (a) $\gamma_-(N)$, and (b) $\gamma_+(N)$, for $\omega = 1.05$ (circles), $\omega = 1.2$ (squares), and $\omega = 1.30$ (triangles). Dashed lines are the results of a fit with Eq. (10). We note that $C_- > 0$ for $\omega = 1.05$, i.e. $\gamma_-(N) \rightarrow \omega^-$ from the left, while $C_- < 0$ for $\omega = 1.20$ and $\omega = 1.30$, i.e. $\gamma_-(N) \rightarrow \omega^+$ from the right. C_+ instead is always positive, i.e., $\gamma_+ \rightarrow 2^-$ from the left. The black dashed line corresponds to a scaling with exponent 1.

IV. GRAPHICALITY OF DOUBLE POWER-LAW SEQUENCES

Consider a double power-law (DPL) distribution defined by

$$p_k = \begin{cases} \frac{k^{-\gamma_1}}{Z_1}, & k_{\min} \leq k \leq k_c(N), \\ \frac{k^{-\gamma_2}}{Z_2}, & k_c(N) \leq k \leq N-1, \end{cases} \quad (11)$$

with $k_c(N) = (N-1)^{1/\omega}$. We also require that

$$\frac{k_c^{-\gamma_1}}{Z_1} = \frac{k_c^{-\gamma_2}}{Z_2} \quad (12)$$

and

$$\sum_{k=k_{\min}}^{N-1} p_k = 1. \quad (13)$$

The first condition tells us that

$$Z_2 = k_c^{-\Delta\gamma} Z_1 = N^{-\frac{\Delta\gamma}{\omega}} Z_1, \quad (14)$$

where $\Delta\gamma = \gamma_2 - \gamma_1$. Setting $Z = Z_1$ we can finally write

$$p_k = \frac{1}{Z} \begin{cases} k^{-\gamma_1}, & k_{\min} \leq k \leq k_c(N), \\ (N-1)^{\frac{\Delta\gamma}{\omega}} k^{-\gamma_2}, & k_c(N) \leq k \leq N-1. \end{cases} \quad (15)$$

See Fig. 3 for a log-log sketch of a DPL distributions with $\gamma_1 > 0$, $\gamma_2 > 0$. By varying ω we can control the tradeoff between the two power-law tails. In particular, for $\omega = 1$ we recover a SPL with exponent γ_1 and $k_c = N-1$, while sending $\omega \rightarrow \infty$ we recover a SPL with exponent γ_2 and an upper cutoff equal to $N-1$. Finally, taking the limit $\gamma_2 \rightarrow \infty$, we recover a SPL with exponent γ_1 and $k_c = (N-1)^{1/\omega}$.

We note that for DPL sequences there are three different types of nodes: finite-degree nodes, hubs (defined

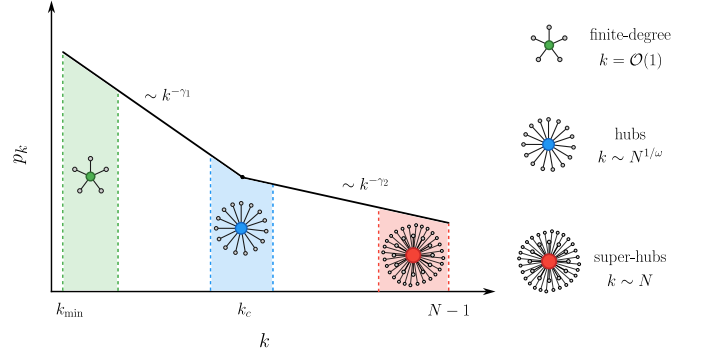


Figure 3. Pictorial visualization of the node classes for DPL distributions. On the left, a schematic log-log plot of a DPL distribution, with the crossover between the two exponent at $k_c \sim N^{1/\omega}$. Shaded regions identify the three distinct classes, defined on the right.

as the nodes with degree of order $k_c(N)$), and superhubs (nodes with degree of order N). See Figure 3 for a pictorial visualization. The number of nodes of each type is $n_{\mathcal{O}(1)}$, $n_{\mathcal{O}(k_c)}$ and $n_{\mathcal{O}(N)}$, respectively. In Appendix D, we present a characterization of the relevant features of these different types of nodes. Fig. 4(a) summarizes the results. In particular, the different filling patterns (corresponding to regions I, II, III) indicate different scalings of the normalization Z , while different labels (Ia, Ib, Ic, IIa, IIb, III) indicate different scalings of the total number of stubs S .

Using these results we can apply again the sufficient conditions for graphicality and nongraphicality.

A. Conditions for graphicality

Cloteaux's inequality, as formulated in Eq. (B4), can be used only where k_{\max} scales slower than N . In such a case, applying Cloteaux's condition we get (see Appendix B for details) that sequences are always graphical for

$$\begin{cases} \gamma_2 > \frac{3\omega-1}{\omega-1}, & \gamma_1 < 1, \\ \gamma_2 > 3 + \frac{2}{\omega-\gamma_1}, & 1 < \gamma_1 < 2, \end{cases} \quad (16)$$

which are subregions of, respectively, (IIa) and (Ib) in Fig. 4(a) above the dashed lines. Contrary to the SPL case, these conditions provide only loose bounds for graphicality, as we show in the next section.

B. Conditions for nongraphicality

Let us start with the case in which superhubs are the dominating nodes, see regions (Ic), (IIb) and (III) of Fig. 4(a).

In region (Ic) the ratio $r_{\mathcal{O}(N)}$ is

$$r_{\mathcal{O}(N)} \sim \frac{N^{\theta_3}}{N^{2\theta_2}} \sim N^{1-\theta_2}, \quad (17)$$

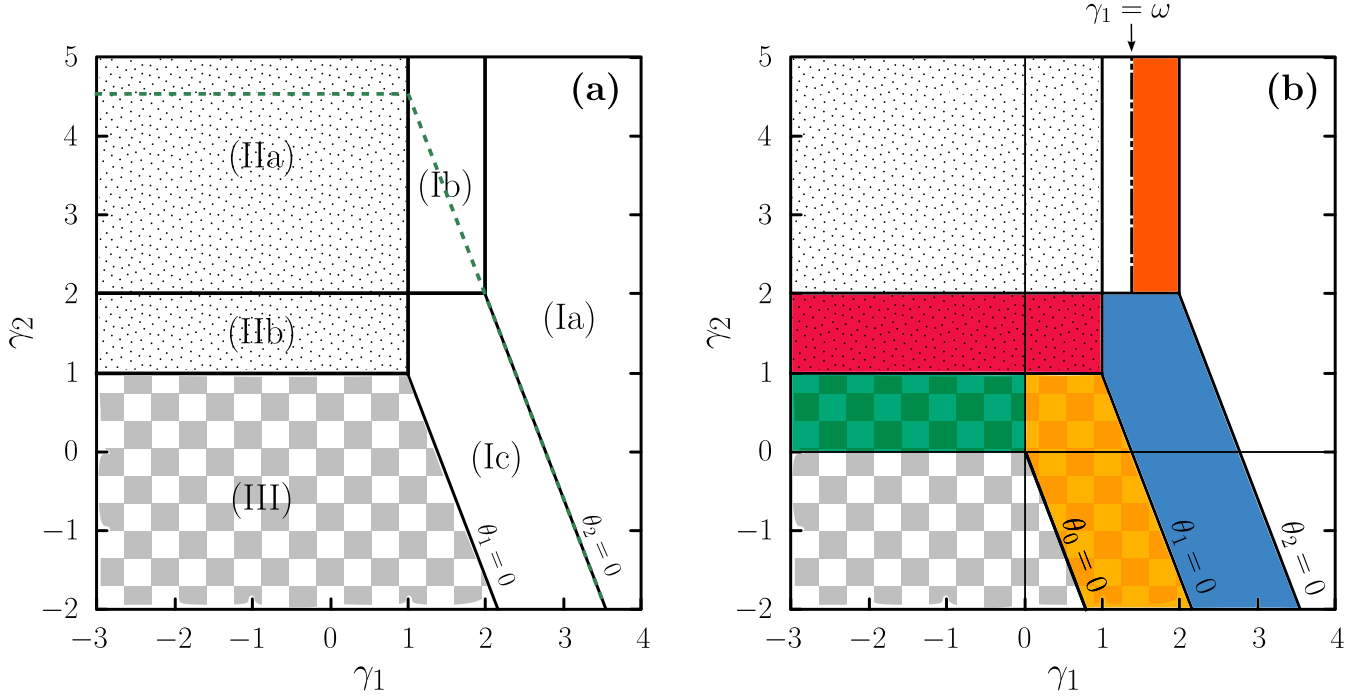


Figure 4. (a) The 6 regions corresponding to different scalings of S determined in Eq. (D14), with different filling patterns (and roman numerals) indicating the different scalings of Z (Eq. (D1)). Below the green dashed lines $k_{\max} \sim N$. Here $\omega = 11/8$. (b) Colors identify regions of nongraphicality. Yellow is caused by the HH condition applied to nodes of degree 1. Green is caused by the HH condition applied to nodes of degree N^α with $\alpha < 1$. Red and blue are caused by an excess of stubs of the superhubs. Orange is caused by an excess of stubs of the hubs.

where

$$\theta_n = \frac{n\omega - (\omega - 1)\gamma_2 - \gamma_1}{\omega}. \quad (18)$$

The ratio diverges since $\theta_2 < 1$. Hence it is not possible to pair stubs among superhubs only and we conclude that sequences are not graphical, see the blue region in Fig. 4(b).

In region (IIb) the ratio is

$$r_{\mathcal{O}(N)} \sim \frac{N^{3-\gamma_2+\frac{\gamma_2-1}{\omega}}}{N^{2[2-\gamma_2+\frac{\gamma_2-1}{\omega}]}} \sim N^{1-\theta_2} = N^{(\gamma_2-1)(1-\frac{1}{\omega})} \quad (19)$$

which diverges as N grows. Again it is not possible to pair stubs among superhubs only. Hence also this region, depicted in red in Fig. 4(b), is nongraphical.

In region (III) instead, there are order N hubs and they emanate order N^2 stubs. The ratio is of order 1. Hence we have no clear indication that this region is nongraphical, however, since the largest degrees are of order N we have to consider also the Havel-Hakimi condition, which predicts nongraphicality if there are nodes with degree of order N , which is true in region (III), and nodes with degree of order N^α . The scaling of \mathcal{N}_{N^α} depends on whether $\alpha > 1/\omega$ or not. Let us first consider $\alpha < 1/\omega$. If $\gamma_1 > 0$, then the worst case scenario happens for $\alpha = 0$, when we consider finite degree nodes. We have

$$Np_1 \sim N^{1-\theta_1} = N^{-\theta_0} \quad (20)$$

which goes to zero only for $\theta_0 > 0$. Hence we can conclude that sequences are not graphical when $\theta_0 < 0$, a region depicted in yellow in Fig. 4(b). Let us now consider $\gamma_1 < 0$. Now the worst case scenario happens for $\alpha \geq 1/\omega$. In region III

$$\mathcal{N}_{N^\alpha} \sim N^{\gamma_2(1-\alpha)}, \quad (21)$$

which is of order (at least) 1 if $\gamma_2 > 0$, no matter the value of α . This implies that sequences cannot be graphical in the intersection between region III and the region where $\gamma_1 < 0, \gamma_2 > 0$. In this way we can conclude that the green region in Fig. 4(b) is nongraphical.

Let us now consider the other regions, where superhubs do not account for the majority of stubs and hence the Havel-Hakimi condition plays no role.

In region (Ia) there are, for large N , practically only nodes of finite degree and order N stubs emanating from them. They can be easily accommodated and graphicality is trivial.

In region (Ib) hubs account for practically all stubs. Is it possible to pair them among themselves? Considering the ratio

$$\frac{S_{\mathcal{O}(k_c)}}{n_{\mathcal{O}(k_c)}^2} \sim \frac{N^{1+\frac{2-\gamma_1}{\omega}}}{N^{2(1+\frac{1-\gamma_1}{\omega})}} \sim N^{-1+\frac{\gamma_1}{\omega}} \quad (22)$$

it turns out that for $\gamma_1 > \omega$ the exponent is positive and the closing of stubs is not possible. Hence a subset

of region (Ib), depicted in orange in Fig. 4(b), is not graphical.

Finally, in region (IIa), we have

$$\frac{S_{\mathcal{O}(k_c)}}{n_{\mathcal{O}(k_c)}^2} \sim \frac{N^{1+\frac{1}{\omega}}}{N^2} \sim N^{-1+\frac{1}{\omega}} \quad (23)$$

The vanishing of this ratio as N increases guarantees that all stubs emanating from hubs can be paired among themselves, providing no indication of nongraphicality.

The complete picture presented in Fig. 4(b) shows a much richer scenario than the SPL case. The tail with exponent γ_2 plays a crucial role not only when $\gamma_2 < 2$, as one could naively expect. As a matter of fact, γ_2 always affects the scaling of k_{\max} , given in Eq. (D6), and only in the limit $\gamma_2 \rightarrow \infty$ we have $k_{\max} \rightarrow k_c$, recovering the SPL case with exponent γ_1 . This is in agreement with our previous results for SPL in Fig. 1(a). The orange region $\omega < \gamma_1 < 2$ exists only for $\omega < 2$. In fact, if $\omega > 2$ our heuristic argument does not predict a nongraphical region in (Ib). For $\omega \rightarrow \infty$ the DPL reduces to a SPL with exponent γ_2 and $k_c = N - 1$. Thus we expect to get the same behavior observed for the SPL with $\omega = 1$, regardless the value of γ_1 . This is indeed what happens, as the slope of the lines $\theta_n = 0$ tends to 0, i.e., they become horizontal. In the other limiting case $\omega \rightarrow 1$, we have a SPL with exponent γ_1 and $k_c = N - 1$. This is in agreement with our picture, as the slope of the lines $\theta_n = 0$ diverges and they become vertical. Nongraphicality in the green region and in the red region for $\gamma_1 < 0$ in Fig. 4(b) is produced by a mechanism that involves the presence of all three classes of nodes. This mechanism is active as soon as $\omega > 1$, but discontinuously disappears as $\omega = 1$. This is in perfect analogy to the SPL case for $0 < \gamma < 1$ and $\omega \rightarrow 1^+$. However, in this limit, where the yellow and blue regions become vertical and the whole region (Ib) is orange, our heuristics does not predict nongraphicality for $0 < \gamma_1 < 1$ and $\gamma_2 > 2$. This is in contrast to the results for SPL with $\omega = 1$. This indicates that our picture is incomplete and that we are missing some mechanism causing nongraphicality in region (Ib) and in part of region (IIa). As we shall see in the next section, this is corroborated by the results of numerical simulations.

C. Comparison with numerical simulations

The arguments above indicate the existence of several domains of nongraphicality in the space spanned by γ_1 and γ_2 , but do not guarantee that in the other regions degree sequences are graphical. To have information on the whole phase-space we determine the graphicality numerically, performing simulations as in the case of single power-law distributed networks. Results are reported in Fig. 5.

From the figure it turns out that, although finite size effects are very strong in some parts of the phase-space, the overall picture presented in the previous section is confirmed in the limit of large N : the nongraphical regions

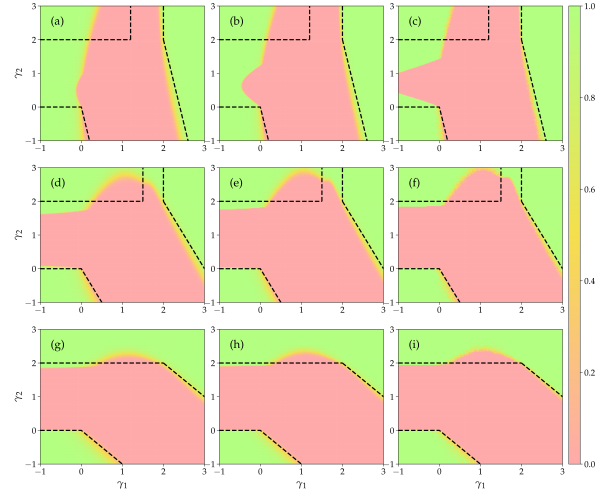


Figure 5. Phase diagram for the graphicality of DPL sequences obtained from numerical simulations sequences of size (a) $N = 10^5$, (b) $N = 10^6$, (c) $N = 10^7$. Colors represent the value of $\langle g \rangle$ as a function of γ_1 and γ_2 for $\omega = 1.20$ (top), $\omega = 1.50$ (middle) and $\omega = 2.00$ (bottom). Results are averaged over $M = 1000$ independent samples for $N = 10^5$, $M = 100$ samples for $N = 10^6$ and $M = 10$ samples for $N = 10^7$. Note the presence of huge finite-size effects.

predicted by the sufficient conditions for nongraphicality turn out to be actually nongraphical in numerical evaluations. The only discrepancy occurs for $0 < \gamma_1 < \omega$, $\gamma_2 > 2$. In this region there seems to exist a nongraphical region not predicted by our arguments. It remains as an interesting direction for further research to understand what is the physical origin of this additional nongraphical domain.

V. DISCUSSION

In this work, we have provided a comprehensive analysis of the graphicality problem for single and double power-law degree sequences with size-dependent cutoffs. By combining exact sufficient conditions with physically-motivated heuristic arguments, we have elucidated the fundamental mechanisms that prevent degree sequences from being graphical.

For single power-law distributions, we have shown that the phase diagram exhibits a rich structure controlled by the interplay between the power-law exponent γ and the cutoff scaling parameter ω , providing a physical picture for the results in Refs. [23, 24]. Our analysis reveals that violations of graphicality may arise from two distinct physical mechanisms: (i) an excess of stubs from high-degree nodes that cannot be matched among themselves, and (ii) the incompatibility between nodes with large degree and finite degree. In particular, (i) always occurs for $\omega < \gamma < 2$, while (ii) arises when there is coexistence of many nodes with degree $\mathcal{O}(N)$ and with degree $\mathcal{O}(1)$,

which happens only for $0 < \gamma < 1$ and $\omega = 1$. The discontinuous behavior for $\omega \rightarrow 1^+$ where $0 < \gamma < 1$ highlights the subtle nature of these constraints.

There is an additional physical consideration, aligned with the stub-scaling argument, which concerns the role of the structural cutoff k_s . The structural cut-off in complex networks marks the degree value beyond which degree-degree correlations necessarily emerge due to graphicality constraints and has been widely studied for single power-law sequences [33]. If the natural cut-off is smaller than the structural cut-off, *i.e.*, $k_{\text{nat}} < k_s$, the degree sequence can be realized as a simple, uncorrelated network. Conversely, if $k_{\text{nat}} > k_s$, such high-degree nodes cannot be realized without intrinsically inducing disassortative degree-degree correlations. For exponent $2 < \gamma < 3$, k_{nat} grows faster than k_s and the structural cut-off becomes a binding constraint, so feasible networks display degree-degree correlations which deter connections among hubs. This is consistent with the stub-scaling rationale presented in Section III, in which hubs preferentially connect to low-degree nodes. On the other hand, when $1 < \gamma < 2$, the network enters an extremely heavy-tailed regime with important structural consequences. Also in this regime, the natural cutoff k_{nat} lies above the structural cutoff k_s . As anticipated above, a simple network can remain uncorrelated only when the largest admissible degree coincides with the structural cutoff. Using the scaling relation of the structural cutoff $k_s^2 \sim N\langle k \rangle \sim Nk_s^{2-\gamma}$, it follows that the maximum degree in simple uncorrelated networks should scale with system size as $k_s \sim N^{1/\gamma}$. As already shown in Ref. [24], this scaling coincides with the upper transition value for graphicality, defining the largest scaling of the imposed cutoff k_c for which the degree sequence can still be realized as a simple graph. Accordingly, for $1 < \gamma < 2$, there is no room for degree-degree correlations to restore graphicality if the imposed cutoff k_c is larger than the structural cutoff k_s , since the degree sequence ceases to be realizable. This contrasts with the case $\gamma > 2$, where the development of disassortative correlations is able to restore graphicality when the imposed cutoff k_c exceeds the structural cutoff k_s .

For double power-law sequences, we have uncovered an even richer phenomenology with five qualitatively different violation mechanisms, each dominating in different regions of the (γ_1, γ_2) parameter space. The transitions between these regions are governed by the interplay between nodes of finite degree, hubs – nodes of degree of order k_c – and superhubs – nodes of degree of order N . This interplay reveals how the competition between the two power-law regimes determines graphicality. Particularly noteworthy is the existence of a non-graphical region for $0 < \gamma_1 < \omega$, $\gamma_2 > 2$ that is not captured by our current heuristic conditions, pointing to additional subtle constraints that merit further investigation. It is also worth to be remarked that Cloteaux's sufficient condition for graphicality is not very useful in this case: in a vast part of the phase-diagram where double power-law sequences are graphical

Cloteaux's condition does not apply. With the benefit of hindsight, this is not surprising, as Cloteaux's condition is based on two scales (k_{min} and k_{max}) while here a third scale k_c plays a relevant role.

Our numerical simulations confirm the theoretical predictions while also revealing surprisingly slow convergence to the infinite-size limit. The finite-size scaling analysis shows that corrections scale logarithmically with system size, explaining why even networks with $N \sim 10^7$ nodes may not fully exhibit the asymptotic behavior. This has important practical implications for the analysis of real-world networks, where finite-size effects cannot be neglected.

The results presented in this work have significant implications for network modeling and generation. The graphicality constraints we identify must be respected when designing synthetic networks or inferring network properties from data. In addition, the presence of hubs and superhubs, and the asymptotic scaling of their stubs may influence the fractality of networks, as captured by the box-covering coarse-graining framework developed in Ref. [34]. Within this framework, fractal networks exhibit finite fractal dimensions as a reflection of hub repulsion, while in non-fractal networks hubs tend to connect to each other. Depending on the parameters, graphicality constraints can force high-degree nodes to connect either to other high-degree nodes or to low-degree ones. These constraints can therefore hinder or foster hub repulsion, suggesting that the structural feasibility of a given degree sequence can intrinsically limit or support the emergence of fractality.

Our findings highlight that not all scale-free networks are sparse: truly dense scale-free networks (with average degree scaling with N) do exist, but only in restricted parameter regimes. These fundamental limits provide important guidance for understanding which network structures are mathematically possible. Future work should address the remaining theoretical gaps in the study of the graphicality of double power-law sequences, in particular the origin of the unexplained non-graphical region, and the characterization and role of the structural cutoff k_s .

VI. ACKNOWLEDGMENTS

C.C. acknowledges the PRIN project No. 20223W2JKJ “WE CARE”, CUP B53D23003880006, financed by the Italian Ministry of University and Research (MUR), Piano Nazionale Di Ripresa e Resilienza (PNRR), Missione 4 “Istruzione e Ricerca” - Componente C2 Investimento 1.1, funded by the European Union - NextGenerationEU. M.A.S. acknowledges support from grant PID2022-137505NB-C22 funded by MCIN/AEI/10.13039/501100011033 and by ERDF/EU. This project has been supported by the FIS 1 funding scheme (SMaC - Statistical Mechanics and Complexity) from Italian MUR (Ministry of University and Research).

Appendix A: Characterization of the single power-law degree distribution

First of all, let us compute the normalization constant,

$$Z = \sum_{k=k_{\min}}^{k_{\max}} k^{-\gamma} \sim \begin{cases} 1, & \gamma > 1, \\ N^{\frac{1-\gamma}{\omega}}, & \gamma < 1. \end{cases} \quad (\text{A1})$$

The number of nodes with finite degrees is proportional to N/Z , and the same holds for number of stubs emanating from nodes of finite degree

$$S_{\mathcal{O}(1)} \sim \frac{N}{Z} \sim \begin{cases} N, & \gamma > 1, \\ N^{1-\frac{1-\gamma}{\omega}}, & \gamma < 1. \end{cases} \quad (\text{A2})$$

Note that this quantity is either linear or sublinear depending on the value of γ and ω .

An important quantity is the so-called natural cutoff k_{\max} , that is the scaling of the largest observed value in a sample of size N generated from Eq. (4). A simple heuristic argument requires

$$\frac{N}{Z} \int_{k_{\max}}^{k_c} dk k^{-\gamma} \sim 1, \quad (\text{A3})$$

from which it follows

$$k_{\max} \sim \begin{cases} N^{\frac{1}{\gamma-1}}, & \omega < \gamma - 1, \\ k_c, & \omega \geq \gamma - 1. \end{cases} \quad (\text{A4})$$

Note that since $\omega \geq 1$, the natural cutoff may play a role only for $\gamma > 2$.

Then we define the hubs, as the nodes with degree between $[\epsilon k_{\max}, k_{\max}]$, where $\epsilon = \mathcal{O}(1)$, $\epsilon < 1$ and $k_{\max} = N^{\frac{1}{\omega}}$. With the same logic as above, we can estimate the average number of hubs as

$$\mathcal{N}_{\mathcal{O}(k_{\max})} = \frac{N}{Z} \sum_{k=\epsilon k_{\max}}^{k_{\max}} k^{-\gamma} \sim \begin{cases} N^{1-\frac{\gamma-1}{\omega}}, & \gamma > 1, \\ N, & \gamma < 1. \end{cases} \quad (\text{A5})$$

Similarly, we can estimate the average number of stubs emanating from the hubs, given by

$$S_{\mathcal{O}(k_{\max})} = \frac{N}{Z} \sum_{k=\epsilon k_{\max}}^{k_{\max}} k^{-\gamma+1} \sim \begin{cases} N^{1-\frac{\gamma-2}{\omega}}, & \gamma > 1, \\ N^{1+\frac{1}{\omega}}, & \gamma < 1. \end{cases} \quad (\text{A6})$$

Finally, the total number of stubs in the system is

$$S = N\langle k \rangle \sim \begin{cases} N, & \gamma > 2, \\ N^{1+\frac{2-\gamma}{\omega}}, & 1 < \gamma < 2, \\ N^{1+\frac{1}{\omega}}, & \gamma < 1. \end{cases} \quad (\text{A7})$$

Appendix B: Cloteaux's inequality in practice

Cloteaux's inequality Eq. (3) can be rewritten as

$$\frac{2k_{\max}^2 N + k_{\min} k_{\max} N + k_{\min}^2 N^2 + k_{\min}(1+k_{\min})S + S^2 - k_{\max}^2 - k_{\max}S - 2k_{\min} k_{\max} N - N k_{\min}^2 - 2S N k_{\min}}{(N k_{\max} - S)(S - N k_{\min})} \geq 0. \quad (\text{B1})$$

Keeping only the leading orders for large N , we get

$$\frac{2k_{\max}^2 N + S^2 - k_{\max}^2 S - 2k_{\min} N S}{(N k_{\max} - S)(S - N k_{\min})} \geq 0 \quad (\text{B2})$$

Since $Nk_{\min} < S < Nk_{\max}$ always, the denominator is positive and we can then write

$$2k_{\max}^2 N + S^2 - k_{\max}^2 S - 2k_{\min} N S \geq 0, \quad (\text{B3})$$

Furthermore, since $k_{\max}^2 N < k_{\max}^2 S$ and $k_{\min} N S < S^2$, the inequality simplifies and reduces to

$$S - k_{\max}^2 \geq 0. \quad (\text{B4})$$

Note that when $\langle k \rangle = \mathcal{O}(1)$ this condition only involves the scaling of k_{\max} with N , and it is equivalent to the ZZ condition Eq. (2) in the large N limit.

1. Cloteaux's inequality for single power-law distributions

For single power-law distributions with $k_c = (N - 1)^{1/\omega}$, Eq. (B4) provides more information than the ZZ condition Eq. (2) only for $\gamma < 2$. From Eq. (A7) we get

$$\begin{cases} N^{1+\frac{2-\gamma}{\omega}} - N^{\frac{2}{\omega}} \geq 0 & 1 < \gamma < 2, \\ N^{1+\frac{1}{\omega}} + N^{\frac{2}{\omega}} \geq 0 & 1 < \gamma. \end{cases} \quad (\text{B5})$$

Comparing the exponents we can conclude that sequences are graphical in the $N \rightarrow \infty$ limit for

$$\begin{cases} \omega > \gamma & 1 < 2 < \gamma, \\ \omega > 1 & 1 < \gamma. \end{cases} \quad (\text{B6})$$

This sufficient condition for graphicality, together with the heuristic sufficient conditions for nongraphicality, allows us to draw the phase diagram in Fig. 1(a).

2. Cloteaux's inequality for double power-law distributions

The general picture for double power-law distributions is extremely more intricate. However, we can use Cloteaux's inequality to provide some insight on the mysterious region $0 < \gamma_1 < 2$, $\gamma_2 > 2$, i.e., region (Ib) and part of region (IIa) in Fig. 4(a).

Let us first notice that in the regions where $k_{\max} \sim N$, see Eq. (D6) and Fig. 4(a), Cloteaux's condition does not apply, because $S \ll N^2$ always, thus inequality (B4) is never satisfied. To use Eq. (B4) we must then stay in the region where $k_{\max} \ll N$. In (Ib) we have $k_{\max} \sim N^{\frac{\omega+\Delta\gamma}{\omega(\gamma_2-1)}}$, from which it follows, using Eq. (B4),

$$1 + \frac{2 - \gamma_1}{\omega} > \frac{2(\omega + \gamma_2 - \gamma_1)}{\omega(\gamma_2 - 1)}. \quad (\text{B7})$$

After some simplifications we get

$$(\omega - \gamma_1)\gamma_2 > 3(\omega - \gamma_1) - 3\gamma_1. \quad (\text{B8})$$

If $\omega < \gamma_1$, the region defined by this inequality lives outside region (Ib), thus we can discard this case. If instead $\gamma_1 < \omega$ we have

$$\gamma_2 > 3 + \frac{2}{\omega - \gamma_1}. \quad (\text{B9})$$

This region is bounded by a vertical asymptote as $\gamma_1 \rightarrow \omega^-$, in agreement with our heuristic criterion for nongraphicality that holds for $\gamma_1 > \omega$, and in agreement with the single power-law case that is recovered for $\gamma_2 \rightarrow \infty$. Concerning region (IIa), we can simply set $\gamma_1 = 1$ to get the condition

$$\gamma_2 > \frac{3\omega - 1}{\omega - 1}. \quad (\text{B10})$$

These regions determined by the Cloteaux's condition are far from the regions determined by our heuristic criteria for nongraphicality, see Fig. 4(b). We can conclude that for the case of double power-law distributions, Cloteaux's inequality provides only a mild upper bound for the graphical regions. Remarkably, for $\omega \rightarrow \infty$ we get $\gamma_2 > 3$, which is exactly the condition for Cloteaux's inequality to be applied for SPL distributions.

Appendix C: Algorithm to perform EG Test for graphicality of degree sequence

In this section, we outline an efficient implementation of the Erdős–Gallai (EG) test in Eq. (1) for determining whether a given ordered non-increasing degree sequence with even sum is graphical [1]. The algorithm, strongly inspired by the one described in Ref. [12], exploits recurrence relations to evaluate the EG inequalities in $\mathcal{O}(N)$ time, improving upon the naive $\mathcal{O}(N^2)$ approach.

Let $\underline{k} = (k_1, \dots, k_N)$ be an ordered, non-increasing degree sequence with even sum. The classical form of the EG test requires checking a series of inequalities

$$L_n \leq R_n, \quad (\text{C1})$$

for all $1 \leq n \leq N$, where

$$\begin{aligned} L_n &= \sum_{i=1}^n k_i, \\ R_n &= n(n-1) + \sum_{i=n+1}^N \min(n, k_i). \end{aligned} \quad (\text{C2})$$

Computing the right-hand side R_n directly for every n would require $\mathcal{O}(N^2)$ operations. A much more efficient approach, as suggested in Ref. [12], is to exploit recursive relations that allow both sides of the inequality to be updated in constant time per iteration.

The left-hand side can be easily obtained incrementally as

$$L_n = L_{n-1} + k_n, \quad (\text{C3})$$

with the initialization $L_1 = k_1$. For the right-hand side, the recurrence relation is less straightforward and reads

$$R_n = R_{n-1} + 2(n-1) - \min(n-1, k_n) + \sum_{i=n+1}^N [\min(n, k_i) - \min(n-1, k_i)], \quad (\text{C4})$$

which needs a little bit of manipulation. First of all, the last term between square brackets sums up to the number of degrees k_i larger or equal to n with index $i > n$. We can identify two cases:

- if $k_n > n-1$ then $\min(n-1, k_n) = n-1$ and the sum in square brackets is different from zero;
- if $k_n \leq n-1$ then $\min(n-1, k_n) = k_n$ and the sum in square brackets is zero, since $k_i < k_n$ for all $i \leq n+1$ and $\sum_{i=n+1}^N [k_i - k_n] = 0$;

It is therefore convenient to introduce, for each n , the number x_n of nodes with degree larger or equal to n . This quantity is sometimes called crossing-index and can also be seen as the index of the last node that has degree larger than n , *i.e.*, $k_i > n$ for all $i \leq x_n$ and $k_i \leq n$ for all $i > x_n$. Since we are dealing with non-increasing degree sequence, the crossing-index can not increase with n and therefore there exist a value n^* such that $x_n \leq n$ for all $n \geq n^*$. Accordingly, $x_{n^*} \leq n^*$ and since \underline{k} is non-increasing $k_{n^*} \leq k_{x_{n^*}}$. Since by definition $k_{x_{n^*}+1} \leq n^*$, then $k_{n^*+1} \leq n^*$ and n^* marks the switch from the first case to the other. In particular, $k_n > n-1$ for all $n \leq n^*$ while $k_n \leq n-1$ for all $n > n^*$. We can then rewrite the recurrence relation in Eq. (C4) as

$$R_n = \begin{cases} R_{n-1} + 2(n-1) - (n-1) + x_n - n = R_{n-1} + x_n - 1 & n \leq n^*, \\ R_{n-1} + 2(n-1) - k_n & n > n^*. \end{cases} \quad (\text{C5})$$

where $x_n - n$ is the number of degrees $k_i > n$ with index $i > n$, assuming $n < n^*$. Finally, comparing L_n and R_n with $n > n^*$ we notice that

$$R_n - L_n = R_{n-1} - L_{n-1} + 2(n-1) - 2k_n \quad (\text{C6})$$

and since $k_n \leq n-1$ the inequality $L_n < R_n$ is automatically satisfied as soon as $L_{n-1} < R_{n-1}$. Therefore there is no need to check the inequalities for $n > n^*$ and the recurrence relation for R_n can be simplified as

$$R_n = R_{n-1} + x_n - 1, \quad (\text{C7})$$

with the initialization $R_1 = N - 1$. The EG test simplifies to checking n^* inequalities of the form in Eq. (C2) that can be computed efficiently through the recursive relations in Eqs. (C3) and (C7) with the corresponding initialization.

By computing the various x_k once in a single pass over the sequence and only up to n^* , the complete EG test on a non-increasing degree sequence can then be carried out in linear time, as shown in Fig. 6.

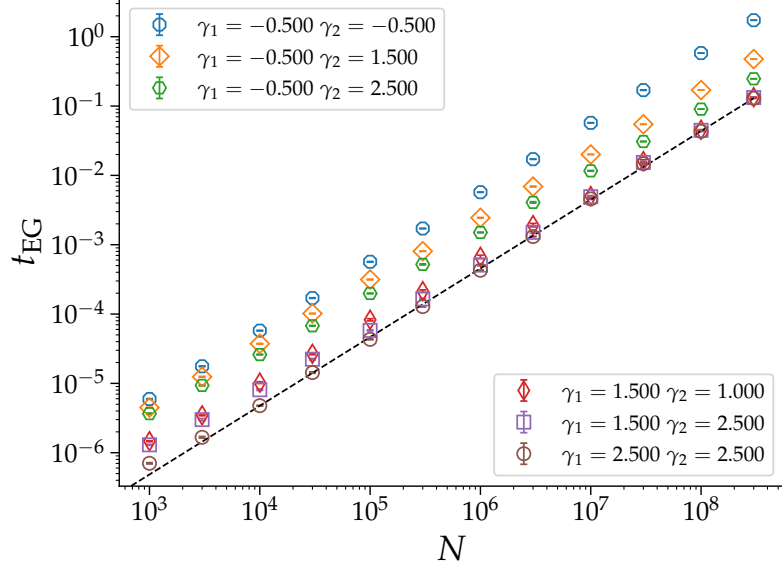


Figure 6. Computation time for the EG test in the form discussed in C for $\omega = 11/8$ and various combination of exponents γ_1 and γ_2 , belonging to the six regions identified in Fig. 4; in particular we employed $\gamma_1 = 2.5, \gamma_2 = 2.5$ (region (Ia)), $\gamma_1 = 1.5, \gamma_2 = 2.5$ (region (Ib)), $\gamma_1 = 1.5, \gamma_2 = 1$ (region (Ic)), $\gamma_1 = -0.5, \gamma_2 = 2.5$ (region (IIa)), $\gamma_1 = -0.5, \gamma_2 = 1.5$ and $\gamma_1 = -0.5, \gamma_2 = -0.5$ (region (III)). Results are averaged over 100 independent sequences.

Appendix D: Characterization of the double power-law degree distribution

1. The normalization

There are three regions, represented using distinct filling patterns in Fig. 4(a), defining the behavior of Z ,

$$Z \sim \begin{cases} 1 & \gamma_1 > 1, \theta_1 < 0 \quad (\text{region I}), \\ N^{\frac{1-\gamma_1}{\omega}} & \gamma_1 < 1, \gamma_2 > 1 \quad (\text{region II}), \\ N^{\theta_1} & \gamma_2 < 1, \theta_1 > 0 \quad (\text{region III}). \end{cases} \quad (\text{D1})$$

where we define in general

$$\theta_n = \frac{n\omega - (\omega - 1)\gamma_2 - \gamma_1}{\omega}. \quad (\text{D2})$$

Note that $\theta_n \pm 1 = \theta_{n\pm 1}$. The curves $\theta_n = 0$ correspond to straight lines in the $\gamma_1 - \gamma_2$ plane, which pass through the point (n, n) . Note that these lines separate domains where $\theta_n < 0$ (above the line) from domains where $\theta_n > 0$ (below the line).

For $\omega \rightarrow 1$, the curves reduce to $\gamma_1 = n$. This is reasonable since we are pushing the crossover up to $N - 1$, hence the tail with exponent γ_2 is not observed and must produce no effect on the graphicality. For $\omega \rightarrow \infty$ instead, these lines become $\gamma_2 = n$. The crossover takes place “sooner” and the distribution feels only the presence of the tail with exponent γ_2 . It is important to note that the larger the value of ω , the more relevant is the effect of the tail with exponent γ_2 .

2. The scaling of largest observed degree k_{\max}

Random numbers generated from a double power-law sequences as defined in Eq. (15) can in principle fluctuate up to $N - 1$. However, depending on the values of γ_1, γ_2 and ω , a natural cutoff emerges, in perfect analogy to the case of single power-law distributions where if no cutoff is imposed, for $\gamma > 2$ we have $k_{\max} \sim N^{\frac{1}{\gamma-1}}$. Again, a heuristic

extreme value theory argument tells us that k_{\max} can be defined setting

$$N \int_{k_{\max}}^N dk p_k = \mathcal{O}(1). \quad (\text{D3})$$

From this equation, it follows

$$\frac{1}{1 - \gamma_2} [k_{\max}^{1 - \gamma_2} - N^{1 - \gamma_2}] \sim Z N^{-1 - \frac{\Delta\gamma}{\omega}}. \quad (\text{D4})$$

If $\gamma_2 < 1$, then Eq. (D3) cannot be satisfied, and k_{\max} must scale as $k_{\max} \sim N$. If instead $\gamma_2 > 1$ we get

$$k_{\max} \sim \begin{cases} N^{\frac{\omega + \gamma_2 - \gamma_1}{\omega(\gamma_2 - 1)}}, & \theta_1 < 0 \quad (\text{region I}), \\ N^{\frac{\omega + \gamma_2 - 1}{\omega(\gamma_2 - 1)}} & \gamma_1 < 1, \gamma_2 > 1 \quad (\text{region II}) \end{cases} \quad (\text{D5})$$

However, we must check whether or not the exponent we get from this scaling argument is smaller than 1, otherwise we get again $k_{\max} \sim N$. Imposing this additional condition, we finally have

$$k_{\max} \sim \begin{cases} N^{\frac{\omega + \gamma_2 - \gamma_1}{\omega(\gamma_2 - 1)}} & \gamma_1 > 1, \theta_2 < 0, \\ N^{\frac{\omega + \gamma_2 - 1}{\omega(\gamma_2 - 1)}} & \gamma_1 < 1, \gamma_2 > \frac{2\omega - 1}{\omega - 1}, \\ N & \text{otherwise.} \end{cases} \quad (\text{D6})$$

The region where $k_{\max} \sim N$ lies below the green dashed line in Fig. 4(a).

3. The number of finite-degree nodes, hubs and superhubs

Let us now consider the number of finite-degree nodes $n_{\mathcal{O}(1)}$, hubs $n_{\mathcal{O}(k_c)}$ – defined as the nodes with degree around $k_c(N)$ – and superhubs $n_{\mathcal{O}(N)}$, nodes with degree around N .

$$n_{\mathcal{O}(1)} \sim \begin{cases} N & \gamma_1 > 1, \theta_1 < 0, \quad (\text{region I}), \\ N^{1 - \frac{1 - \gamma_1}{\omega}} & \gamma_1 < 1, \gamma_2 > 1, \quad (\text{region II}), \\ N^{-\theta_0} & \gamma_2 < 1, \theta_1 > 0, \quad (\text{region III}), \end{cases} \quad (\text{D7})$$

$$n_{\mathcal{O}(k_c)} \sim \begin{cases} N^{1 + \frac{1 - \gamma_1}{\omega}} & \gamma_1 > 1, \theta_1 < 0, \quad (\text{region I}), \\ N & \gamma_1 < 1, \gamma_2 > 1, \quad (\text{region II}), \\ N^{\frac{(\omega - 1)\gamma_2 + 1}{\omega}} & \gamma_2 < 1, \theta_1 > 0 \quad (\text{region III}), \end{cases} \quad (\text{D8})$$

$$n_{\mathcal{O}(N)} \sim \begin{cases} N^{\theta_2} & \gamma_1 > 1, \theta_1 < 0, \quad (\text{region I}), \\ N^{2 - \gamma_2 + \frac{\gamma_2 - 1}{\omega}} & \gamma_1 < 1, \gamma_2 > 1, \quad (\text{region II}), \\ N & \gamma_2 < 1, \theta_1 > 0 \quad (\text{region III}). \end{cases} \quad (\text{D9})$$

Note that the number of superhubs in Eq. (D9) is at least finite only for $\theta_2 < 0$ in region I, and for $\gamma_2 > (2\omega - 1)/(\omega - 1)$, in agreement with the scaling of k_{\max} given in Eq. (D6). Otherwise, superhubs do not exist.

4. The number of stubs emanating from finite-degree nodes, hubs and superhubs

We want now to determine the number of stubs emanating from nodes $\mathcal{O}(1)$, $\mathcal{O}(k_c)$ and $\mathcal{O}(N)$, respectively. Note that we have

$$S_{\mathcal{O}(N^\alpha)} \sim N^\alpha n_{\mathcal{O}(N^\alpha)}, \quad (\text{D10})$$

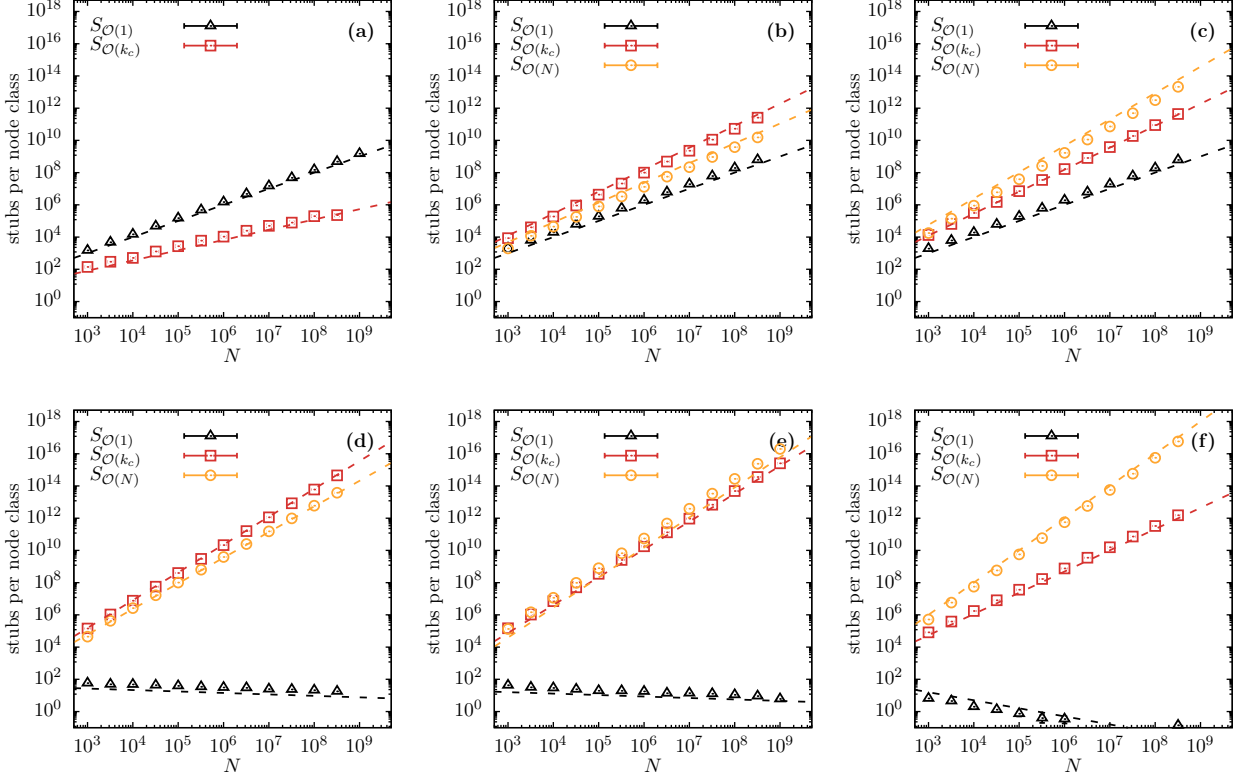


Figure 7. Comparison between numerical evaluation of the stubs emanating from finite-degree nodes (triangles), hubs (squares), and superhubs (circles), and the scaling predictions given in Eqs. (D11)-(D13) (dashed lines). In practice, finite-degree nodes are identified as nodes with $k \in [k_{\min}, c_1 k_{\min}]$, hubs as nodes with $k \in [c_2 k_c, c_3 k_c]$, and superhubs as nodes with degree $k \in [c_4(N-1), N-1]$, with c_1, c_2, c_3, c_4 finite constants. In particular, we used $c_1 = 10$, $c_2 = 1/3$, $c_3 = 3$, $c_4 = 1/3$. The asymptotic scaling is independent on the particular choice of these numbers. We set $\omega = 11/8$ and (a) $\gamma_1 = 2.5$, $\gamma_2 = 2.5$ (region (Ia)), (b) $\gamma_1 = 1.5$, $\gamma_2 = 2.5$ (region (Ib)), (c) $\gamma_1 = 1.5$, $\gamma_2 = 1$ (region (Ic)), (d) $\gamma_1 = -0.5$, $\gamma_2 = 2.5$ (region (IIa)), (e) $\gamma_1 = -0.5$, $\gamma_2 = 1.5$, (f) $\gamma_1 = -0.5$, $\gamma_2 = -0.5$ (region (III)). Results are averaged over 100 independent sequences.

hence

$$S_{\mathcal{O}(1)} \sim \begin{cases} N & \gamma_1 > 1, \theta_1 < 0, \quad (\text{region I}), \\ N^{1-\frac{1-\gamma_1}{\omega}} & \gamma_1 < 1, \gamma_2 > 1, \quad (\text{region II}), \\ N^{-\theta_0} & \gamma_2 < 1, \theta_1 > 0 \quad (\text{region III}). \end{cases} \quad (\text{D11})$$

and

$$S_{\mathcal{O}(k_c)} \sim \begin{cases} N^{1+\frac{2-\gamma_1}{\omega}} & \gamma_1 > 1, \theta_1 < 0, \quad (\text{region I}), \\ N^{1+\frac{1}{\omega}} & \gamma_1 < 1, \gamma_2 > 1, \quad (\text{region II}), \\ N^{\frac{(\omega-1)\gamma_2+2}{\omega}} & \gamma_2 < 1, \theta_1 > 0 \quad (\text{region III}). \end{cases} \quad (\text{D12})$$

and

$$S_{\mathcal{O}(N)} \sim \begin{cases} N^{\theta_3} & \gamma_1 > 1, \theta_1 < 0, \quad (\text{region I}), \\ N^{3-\gamma_2+\frac{\gamma_2-1}{\omega}} & \gamma_1 < 1, \gamma_2 > 1, \quad (\text{region II}), \\ N^2 & \gamma_2 < 1, \theta_1 > 0 \quad (\text{region III}). \end{cases} \quad (\text{D13})$$

As already noted above, the scaling in Eq. (D13) must also be compared with Eq. (D6), in order to guarantee the existence of superhubs. The asymptotic predictions in Eqs. (D11)-(D13) are confirmed by comparison with numerical simulations, as shown in Fig. 7.

5. The total number of stubs

The total number of stubs $S = N\langle k \rangle$ is

$$S \sim \begin{cases} N & \gamma_1 > 2, \theta_2 < 0 \quad (\text{region Ia}), \\ N^{1+\frac{2-\gamma_1}{\omega}} & 1 < \gamma_1 < 2, \gamma_2 > 2 \quad (\text{region Ib}), \\ N^{1+\frac{1}{\omega}} & \gamma_1 < 1, \gamma_2 > 2 \quad (\text{region IIa}), \\ N^{\theta_3} & \gamma_1 < 2, \gamma_2 > 1, \theta_1 < 0, \theta_2 > 0 \quad (\text{region Ic}), \\ N^{3-\gamma_2+\frac{\gamma_2-1}{\omega}} & \gamma_1 < 1, 1 < \gamma_2 < 2 \quad (\text{region IIb}), \\ N^2 & \gamma_2 < 1, \theta_1 > 0 \quad (\text{region III}). \end{cases} \quad (\text{D14})$$

See Fig. 4(a) for a visualization of these regions. By comparing the expressions for S and those for the various types of nodes it is clear that the total number of stubs is dominated by

1. fixed-degree nodes in region (Ia);
2. hubs in regions (Ib) and (IIa);
3. superhubs in regions (IIb), (Ic) and (III).

6. The number of nodes with a given degree

Let us compute the number of nodes with degree N^α . Obviously this number depends on whether α is smaller or larger than $1/\omega$, i.e., whether the degree belongs to the first or to the second power-law of the degree distribution.

$$\mathcal{N}_{N^\alpha} \sim \begin{cases} Z^{-1}N^{1-\alpha\gamma_1} & (0 \leq \alpha < 1/\omega) \sim \begin{cases} N^{1-\alpha\gamma_1} & (\text{region I}) \\ N^{1-\alpha\gamma_1-\frac{1-\gamma_1}{\omega}} & (\text{region II}) \\ N^{1-\alpha\gamma_1-\theta_1} = N^{\gamma_2(1-1/\omega)-\gamma_1(\alpha-1/\omega)} & (\text{region III}) \end{cases}, \\ Z^{-1}N^{1+\frac{\Delta\gamma}{\omega}-\alpha\gamma_2} & (1/\omega < \alpha \leq 1) \sim \begin{cases} N^{1+\frac{\Delta\gamma}{\omega}-\alpha\gamma_2} & (\text{region I}) \\ N^{1+\frac{\Delta\gamma}{\omega}-\alpha\gamma_2-\frac{1-\gamma_1}{\omega}} & (\text{region II}) \\ N^{1+\frac{\Delta\gamma}{\omega}-\alpha\gamma_2-\theta_1} = N^{\gamma_2(1-\alpha)} & (\text{region III}) \end{cases} \end{cases} \quad (\text{D15})$$

[1] P. Erdős and T. Gallai, Graphs with prescribed degrees of vertices, *Mat. Lapok* **11**, 264 (1960).

[2] G. Sierksma and H. Hoogeveen, Seven criteria for integer sequences being graphic, *Journal of Graph Theory* **15**, 223 (1991).

[3] A. Tripathi and H. Tyagi, A simple criterion on degree sequences of graphs, *Discrete Applied Mathematics* **156**, 3513 (2008).

[4] A. Iványi, L. Lucz, T. Móri, and P. Sótér, On erdős-gallai and havel-hakimi algorithms, *Acta Universitatis Sapientiae Informatica* **3**, 230 (2011).

[5] M. A. Rodríguez, Graphicality conditions for general scale-free complex networks and their application to visibility graphs, *Phys. Rev. E* **94**, 012314 (2016).

[6] D. Burstein and J. Rubin, Sufficient conditions for graphicality of bidegree sequences, *SIAM Journal on Discrete Mathematics* **31**, 50 (2017).

[7] M. Ritchie, L. Berthouze, and I. Z. Kiss, Generation and analysis of networks with a prescribed degree sequence and subgraph family: higher-order structure matters, *Journal of complex networks* **5**, 1 (2017).

[8] M. D. Barrus, The principal erdős–gallai differences of a degree sequence, *Discrete Mathematics* **345**, 112755 (2022).

[9] A. Bar-Noy, T. Böhnlein, D. Peleg, M. Perry, and D. Rawitz, Relaxed and approximate graph realizations, in *Combinatorial Algorithms*, edited by P. Flocchini and L. Moura (Springer International Publishing, Cham, 2021) pp. 3–19.

[10] M. Molloy and B. Reed, A critical point for random graphs with a given degree sequence, *Random structures & algorithms* **6**, 161 (1995).

[11] M. Molloy and B. Reed, The size of the giant component of a random graph with a given degree sequence, *Combinatorics, Probability and Computing* **7**, 295 (1998).

[12] C. I. Del Genio, H. Kim, Z. Toroczkai, and K. E. Bassler, Efficient and exact sampling of simple graphs with given arbitrary degree sequence, *PloS one* **5**, e10012 (2010).

[13] B. Bollobás, A probabilistic proof of an asymptotic formula for the number of labelled regular graphs, *European Journal of Combinatorics* **1**, 311 (1980).

[14] H. Kim, Z. Toroczkai, P. L. Erdős, I. Mikl'os, and L. A. Sz'ekely, Degree-based graph construction, *Journal of Physics A: Mathematical and Theoretical* **42**, 392001 (2009).

[15] F. Viger and M. Latapy, Efficient and simple generation of random simple connected graphs with prescribed degree sequence, *Journal of Complex Networks* **4**, 15 (2016).

[16] T. Britton, M. Deijfen, and A. Martin-Löf, Generating simple random graphs with prescribed degree distribution, *Journal of statistical physics* **124**, 1377 (2006).

[17] F. Chung and L. Lu, Connected components in random graphs with given expected degree sequences, *Annals of combinatorics* **6**, 125 (2002).

[18] M. Bayati, J. H. Kim, and A. Saberi, A sequential algorithm for generating random graphs, *Algorithmica* **58**, 860 (2010).

[19] F. van Ieperen and I. Kryven, Sequential stub matching for asymptotically uniform generation of directed graphs with a given degree sequence: F. van ieperen and i. kryven, *Annals of Combinatorics* **29**, 227 (2025).

[20] C. Greenhill, Generating graphs randomly, in *Surveys in Combinatorics 2021*, London Mathematical Society Lecture Note Series, edited by K. K. Dabrowski, M. Gadouleau, N. Georgiou, M. Johnson, G. B. Mertzios, and D. Paulusma (Cambridge University Press, 2021) p. 133–186.

[21] V. Havel, Poznámka o existenci konečných grafu, *Casopis pro pestování matematiky* **80**, 477 (1955).

[22] S. L. Hakimi, On realizability of a set of integers as degrees of the vertices of a linear graph. i, *Journal of the Society for Industrial and Applied Mathematics* **10**, 496 (1962).

[23] C. I. Del Genio, T. Gross, and K. E. Bassler, All scale-free networks are sparse, *Phys. Rev. Lett.* **107**, 178701 (2011).

[24] Y. Baek, D. Kim, M. Ha, and H. Jeong, Fundamental structural constraint of random scale-free networks, *Phys. Rev. Lett.* **109**, 118701 (2012).

[25] M. Mitzenmacher, A brief history of generative models for power law and lognormal distributions, *Internet Mathematics* **1**, 226 (2004).

[26] Qian, Jiang-Hai, Li, Hui-Fang, Yang, Chao, and Han, Ding-Ding, Double power-law distribution in spatial network induced by cost constraints, *EPL* **142**, 31002 (2023).

[27] W. Li and X. Cai, Statistical analysis of airport network of china, *Phys. Rev. E* **69**, 046106 (2004).

[28] C. M. Pinto, A. M. Lopes, and J. Tenreiro Machado, Double power laws, fractals and self-similarity, *Applied Mathematical Modelling* **38**, 4019 (2014).

[29] A. A. Toda, Income dynamics with a stationary double pareto distribution, *Phys. Rev. E* **83**, 046122 (2011).

[30] H. Li, E. Valdés, and E. Vives, Double power-law universal scaling function for the distribution of waiting times in labquake catalogs, *Phys. Rev. E* **110**, 064140 (2024).

[31] I. E. Zverovich and V. E. Zverovich, Contributions to the theory of graphic sequences, *Discrete Mathematics* **105**, 293 (1992).

[32] B. Cloteaux, A sufficient condition for graphic sequences with given largest and smallest entries, length, and sum, *Discrete Mathematics & Theoretical Computer Science* **Vol. 20 no. 1**, 25 (2018).

[33] M. Boguná, R. Pastor-Satorras, and A. Vespignani, Cut-offs and finite size effects in scale-free networks, *The European Physical Journal B* **38**, 205 (2004).

[34] C. Song, S. Havlin, and H. A. Makse, Origins of fractality in the growth of complex networks, *Nature physics* **2**, 275 (2006).